Distributed Adaptive Control Strategy for Microgrids Considering Disturbance Effects

Ma L., Xu G., Tan Y.

1. Hunan Communication Polytechnic, Changsha 410132, China

2. School of Traffic& Transportation Engineering, Changsha University of Science & Technology, Changsha 410014, China

3. Key Laboratory of Road Structure and Materials Transportation Industry (Research Institute of Highway Ministry of Transport), Beijing 100088, China

ABSTRACT

In this paper, the physical and mechanical properties of TISCO steel slag were tested by different ratios of composite activators. The optimal neutral composite activator was determined, and the properties of neutral activated steel slag power-cement composite cementitious material with 30% cement content were studied. The experimental results indicated that the best ratio of gypsum: silica fume: sodium sulfate: sodium aluminate: self-made activator was 2.5:2.5:1:0.5:0.5. Through XRD, SEM and TG-DTG detection, less stable periclase was found at 30% cement content and activated steel slag slurry. After 28d curing, the micro morphology and compactness of hydration products were not different from those of cement, and there were even no incompletely hydrated particles. The voids between hydration products and the interface of different hydration products were continuously filled with hydration products over age. C-S-H and AFt generated by 7d activated SSP cement composite powder was greater than those of cement. At 28d, a small amount of $Ca(OH)_2$ was generated. The results show that the combination of self-made neutral activator and other activators can improve the properties of cement steel slag powder composite cementitious material and improve the utilization rate of steel slag.

1. INTRODUCTION

Steel slag is a by-product discharged from the steel making process. According to different production processes and stages, steel slag is mainly divided into basic oxygen furnaces steel slag (BOF), electric arc furnace slag (EAF), and ladle furnace slag (LF) [1]. The characteristics of steel slag depend on the steel-making process [2]. It is characterized by rich free calcium oxide/magnesium, low gelling performance, high heavy metals and poor volume stability [3-5]. It is industrial solid waste, and its generation rate is about 12%-20%. Till now, China has accumulated more than 1 billion tons of steel slag.

However, the comprehensive utilization rate of steel slag is less than 10%, far from reaching 79% of solid waste in 2025. Reasonable and large consumption of steel slag has unprecedented significance for resource recycling and environmental protection [6]. Solving the disposal problem and improving the utilization rate of steel slag has become the focus of solid waste disposal at this stage.

Under the action of activator and hydration medium, the hydraulic minerals in steel slag will react to form new hardened bodies, such as $Ca(OH)_2$, C-S-H, and hydrated calcium aluminate [7]. Many experts have studied how to effectively apply steel slag to cement and concrete. Its application is limited due to the fact that cement active substances are less than that of cement, and the activities of C_2S and C_3S are low. Another reason is that f-CaO causes volume expansion after water absorption. Natural aging eliminates the need to store steel slag in the slag yard, which is difficult to implement due to its large footprint and long storage time. Nunes and Borges [8] pointed out that steel slag was an alternative material for Portland cement. The research is still in the primary stage, but promising. In this way, inhibiting the late expansion of steel slag is one of the key problems to be solved in the utilization of steel slag.

Due to the potential cementitious properties of steel slag, Li et al. [9-10] studied the workability and mechanical properties of concrete with different additions of steel slag, so as to make it a cement mixture that partially replaces cement. Replacing cement with steel slag can increase the workability of concrete, but the compressive strength decreases with the increase of the content. Parron-Rubio et al. [11] found that when steel slag from different sources replaced 25% of the cement, the properties of concrete would change. (Raheem et al. [12] studied the effect of different water-cement ratios on the strength of recycled steel slag aggregate concrete. It was found that low water-cement ratio can improve the compressive and flexural strength of concrete. Huang et al. [13] studied the shrinkage characteristics of calcium sulphoaluminate cement with different additions of steel slags. They found that the shrinkage rate decreased with the increasing additions of steel slags. Miah et al. [14] studied the mechanical strength, shrinkage and durability of mortars made of different additions of SSP at two water cement ratios before and after high temperatures (120 ℃, 250 ℃, 400 ℃ and 600 ℃). It was found that the mortar containing SSP had higher mechanical strength and better durability.

In order to improve the volume stability and mechanical properties of steel slag concrete, Zhou et al. [15] found that pre-grinding could dissociate part of f-CaO that solid-dissolved in the refractory phase. Morone et al. and Fang et al. [16-17] studied that CO_2 pretreatment of steel slag can improve the compressive strength and volume stability of mortar. Shen et al. [18] prepared pervious concrete with carbonated steel slag powder as binder and crushed steel slag as aggregate and applied it in the construction of Sponge City. However, stable pretreatment leads to increased costs and other environmental problems [19]. Sun et al. [20] studied the activation effect of sodium silicate on steel slag and found that the hydration reaction and products of activated steel slag were similar to those of cement. Its compressive strength was only 30%-40% of that of Portland cement. Guan et al. [21] found that activator was the main factor affecting cement mortar mixed with steel slag. Through establishing a GM (0, N) prediction model, it was proposed that activated steel slag powder (SSP) could partially replace the cement and reduce the cost of cementitious materials, but there were a loss of strength. Martins et al. [5] prepared cement-based composites with good mechanical properties and durability with activated SSP, encouraging further research to popularize the utilization rate of steel slag.

Scholars have done relevant researches on replacing cement with steel slag, using activators to promote steel slag hydration and improve the properties of SSP cementitious materials. In most activators, the compounds that promote the hydration of steel slag are single, and the promoting effect of composite activators cannot be fully exerted. In this paper, the self-made neutral activator is compounded with other activators to determine the best ratio of neutral composite activator, so as to effectively improve the performance of cement steel slag powder cementitious material and improve the utilization rate of steel slag.

2. EXPERIMENTS

2.1 Raw materials

2.1.1. Cement

The cement clinker was Shanxi Jinpai P.S.A 32.5 cement in China, and its properties are shown in Table 1.

Table 1 Physical properties and main chemical compositions of Shanxi Jinpai P.S.A 32.5 cement

Specific Surface Area m^2/kg	**Density g/cm^3**	**CaO**	**MgO**	**SiO_2**	**Al_2O_3**	**Fe_2O_3**
351	3.08	62.7	3.81	24.6	4.51	3.25

2.1.2. Steel slag powder (SSP)

SSP was from the Taiyuan Iron and steel company after iron removal and grinding. The main characteristics are shown in Table 2. The basicity coefficient is an important index for evaluating the gelling activity of SSP. The higher the value, the higher the hydration activity. The basicity coefficient of this steel slag powder is R=2.15, which belongs to high basicity slag.

Table 2 Physical properties and main chemical composition of steel slag powder

Specific Surface Area m^2/kg	**Density g/cm^3**	**CaO**	**MgO**	**SiO_2**	**Al_2O_3**	**Fe_2O_3**
401	3.35	40.6	5.9	17.2	5.5	17.5

The chemical composition of TISCO steel slag powder is shown in Table 2. The contents of CaO and SiO_2 were high with 40.6% and 17.2%, respectively. The contents of CaO and SiO_2 were lower than those of cement.

2.1.3. Activators

The types of activators are shown in Table 3. ZJ were self-made activators. The activators were first compounded in proportion and mixed with steel slag powder in a small ball mill for 20min, so that the activators were evenly distributed to obtain the activated steel slag powder.

Table 3 Activators

Name	Name
a	Gypsum
b	Silica fume
c	Sodium sulfate
d	Sodium aluminate
e	Sodium carbonate
f	ZJ_1 ZJ_2 ZJ_3

2.2 Design of composite activators ratios

Different activators have different effects on the properties of steel slag powder. Gypsum and silica fume have the most obvious effect, followed by sodium sulfate. Sodium aluminate and sodium carbonate can enhance the later strength, and three self-made activators can solve the influence of stability. In order to determine the best composite activator, based on a single activator, the proportion of silica fume and gypsum was fixed, and the mixing ratio and types of other activators were changed. Through the physical and mechanical property test of steel slag powder with different proportion of activator, the best ratio of composite activator was determined. The different experimental ratios of composite activators are shown in Table 4.

Table 4 Experimental ratios of composite activators

Name	Composition of activators	Experimental group
a	a:b:c:d:f_1	A_1 A_2 A_3
b	a:b:c:d:f_2	B_1 B_2 B_3
c	a:b:c:d:f_3	C_1 C_2 C_3
d	a:b:c:e:f_1	D_1 D_2 D_3
e	a:b:c:e:f_2	E_1 E_2 E_3
f	a:b:c:e:f_3	F_1 F_2 F_3

Note: In the A-F experimental groups, the mixture ratios of Group 1, 2 and 3 are 2.5:2.5:1:0.5:0.5, 2.5:2.5:0.5:1:0.5 and 2.5:2.5:1:0.5:0, respectively.

2.3 Experiment and test

After determining the best composite activator, cement and composite activated steel slag powder (7:3) were mixed and milled for 20min to obtain cementitious material. Then 150g of cementitious material was weighted and a certain proportion of composite activator was added to mix manually. Finally, a 2cm×2cm×2cm slurry sample was formed by using the fixed water consumption method (w/c was 0.28). After 24h demolding, it was cured in 20℃ water to the specified ages for physical and mechanical property tests. The samples of activated SSP and cement slurry were cured to the specified age to take out and remove the possible carbonization layer on the surface of the sample. The anhydrous alcohol was added to the selected 5mm internal sample to stop hydration. One part was used to prepare SEM samples, and the other part was ground to certain fineness. They were dried to a constant weight in a 40℃ constant temperature blast drying oven and sealed for storage, then used to prepare XRD test and differential thermal analysis samples.

D8 ADVANCEX-ray diffractometer was used for phase composition analysis. JSM-649LV scanning electron microscope was used for the microstructure and morphology of hydration products. NETZSCH STA449F3 synchronous thermal analyzer was used for the heat and mass changes.

3. EXPERIMENTAL RESULTS AND ANALYSIS

3.1 Effect of activators ratios on the mechanical properties of cement-SSP composite cementitious materials

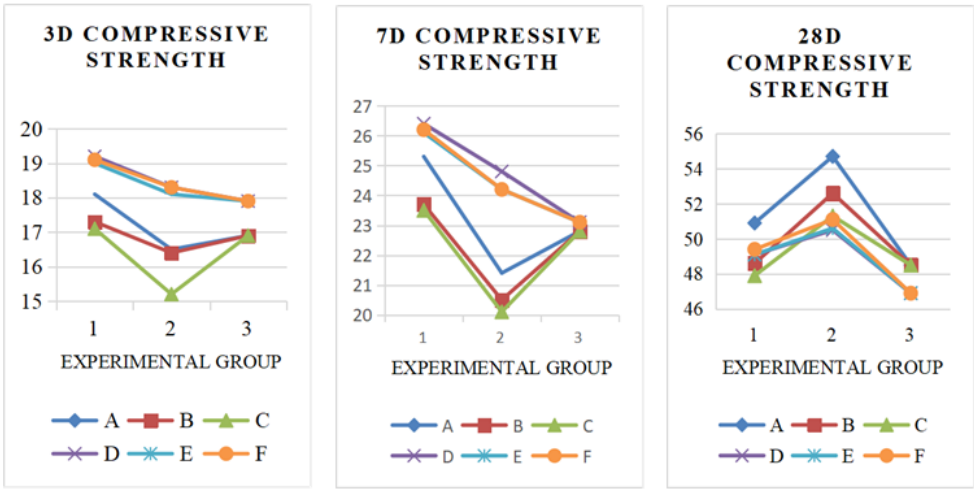

Fig. 1 Effect of activators ratios on the compressive strength of cement-SSP neat mortar (Unit: MPa)

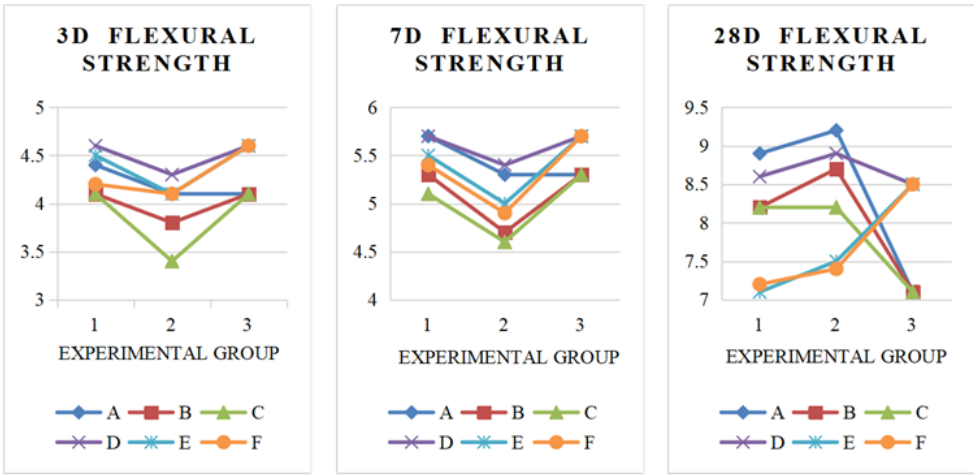

Fig. 2 Effect of activators ratios on the flexural strength of cement-SSP neat mortar (Unit: MPa)

It can be seen from Fig. 1-4 that in the A-F groups of formulas, the content of gypsum and silica fume remained unchanged, and the types and contents of sodium sulfate, sodium aluminate and self-made activator were changed. Gypsum activator mainly provides calcium ions and active hydration products, while silica fume activator had high activity and can accelerate the hydration rate. In the six groups of formulas, the strength of No. 1 was greater than that of the remaining.

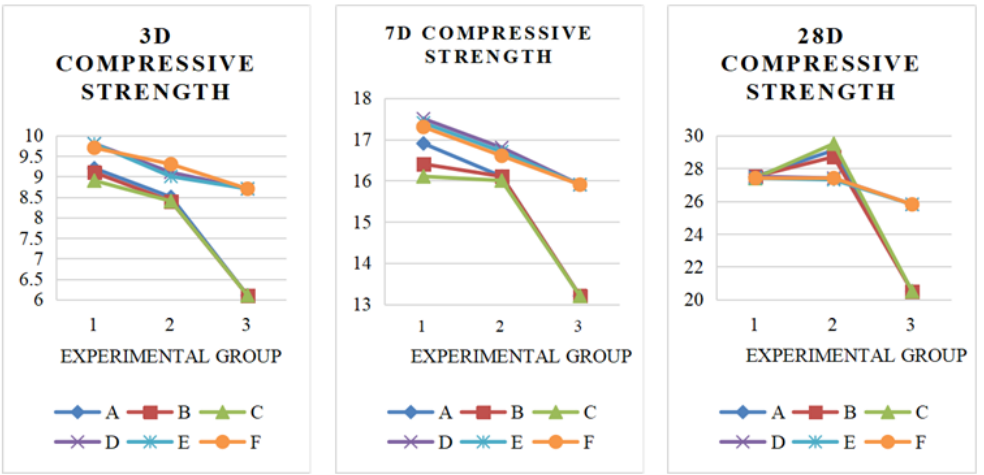

Fig. 3 Effect of activators ratios on the Compressive strength of cement-SSP mortar (Unit: MPa)

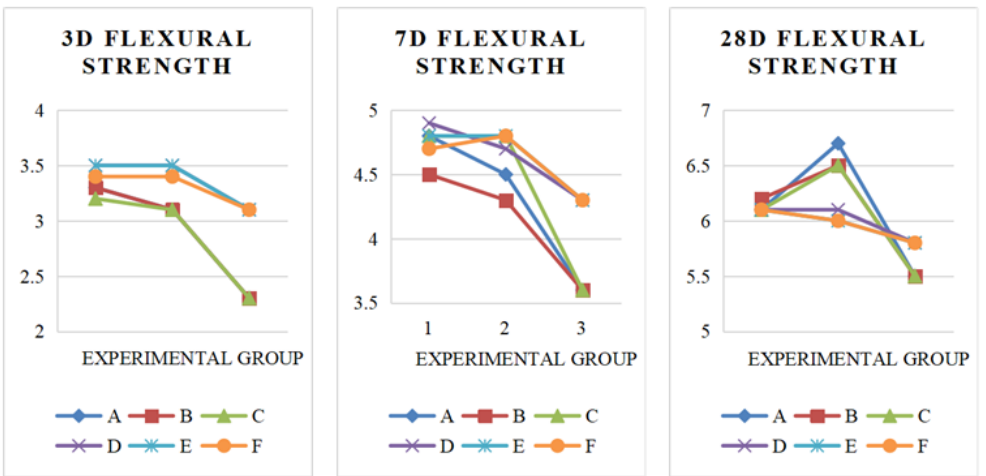

Fig. 4 Effect of activators ratios on the Flexural strength of cement-SSP mortar (Unit: MPa)

It can be seen from A1-A3 that when the content of sodium aluminate increased from 0.5% to 1%, the 3d slurry strength of activated SSP decreased from 18.1MPa to 16.5MPa. 7d decreased from 25.3MPa to 21.4MPa, and 28d increased from 50.9MPa to 54.7MPa. It

showed that sodium aluminate did not significantly improve the early strength, and even decreased with the increase of content. However, the strength was greatly improved in the later stage. It was mainly because it has strong hydrolysis and can absorb a large amount of water in the system, resulting in a certain impact on the early hydration rate of activated SSP. Without self-made activator, when the content of sodium aluminate was 0.5%, the strength in the front and later stages was lower than that when 0.5% self-made activator was added. When the content of sodium sulfate and sodium aluminate remained unchanged and the self-made activator changed from F1 to F2 and F3, the strength decreased. It showed that the self-made activator can enhance the later strength of SSP. Among the three self-made activators, F1 had the greatest effect on the strength. The changes of flexural and compressive strength of activated SSP mortar with different activators were similar to those of neat slurry.

Based on the analysis of the effect of different ratios of activators on the physical and mechanical properties of SSP, the activation effect of A1 composite activator was better. The final ratio of gypsum, silica fume, sodium sulfate, sodium aluminate and self-made activator was 2.5:2.5:1:0.5:0.5.

3.2 Hydrate phase analysis of SSP cement composite powder and SSP slurry

3.2.1 Phase analysis of hydration sample of SSP cement composite cementitious materials

Fig. 5 (a) and Fig. 5 (b) show the XRD results of 7d and 28d hydration of activated SSP cement composite powder slurry, respectively. It can be seen that the types of minerals generated at different ages were similar, and the characteristic peaks were different. From 7d to 28d age, the peak values of hydration products such as $Ca(OH)_2$, AFt and C-S-A gel increased, and the

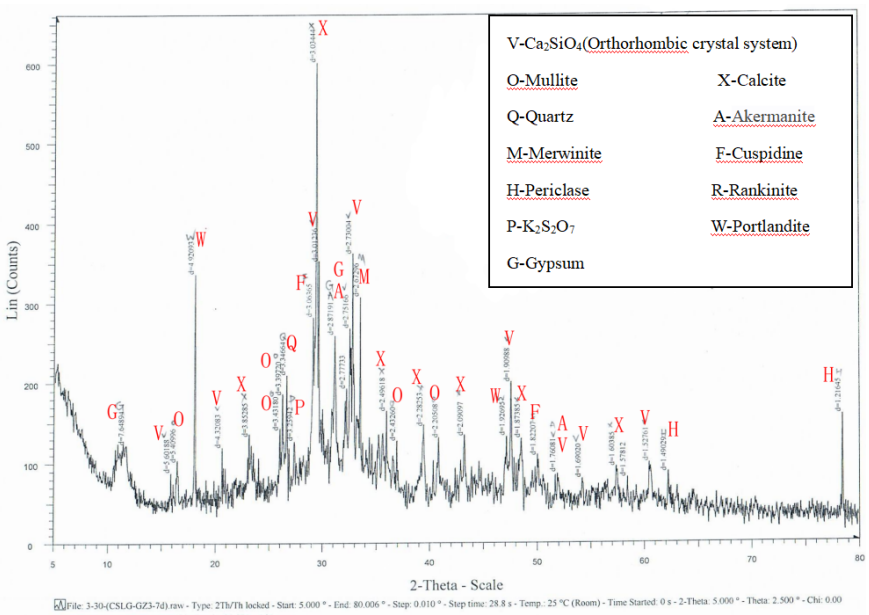

(a) XRD diagram of 7d hydration of activated steel slag powder cement composite powder slurry

peak values of incomplete hydration minerals such as gypsum and calcite decreased. Compared with activated SSP slurry, the peak values of the same minerals at the same age were low, and a new mineral characteristic peak of hydration product $Ca(OH)_2$ appeared. The characteristic peak of gypsum minerals may be the hydration products or the residue in unreacted activators. In general, the hydration degree of activated SSP cement composite powder slurry was higher than that of activated SSP slurry.

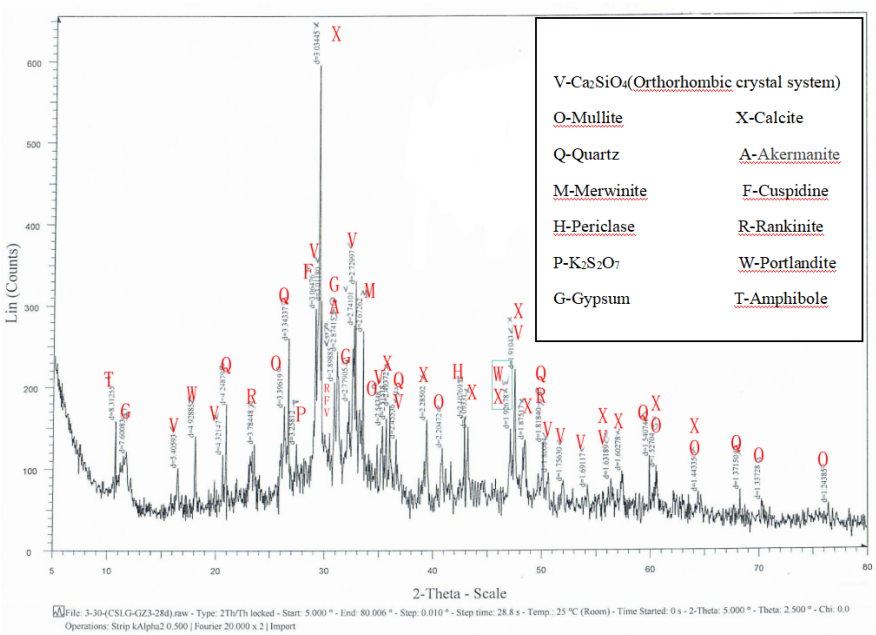

(b) XRD diagram of 28d hydration of activated steel slag powder-cement composite powder slurry

Fig. 5 XRD diagram of hydration products of activated steel slag powder cement composite powder slurry

3.2.2 Phase analysis of hydration sample of steel slag powder cement slurry

Fig. 6 (a) and (b) are the XRD diagrams of 7D and 28d hydration of activated SSP slurry, respectively. It can be seen that the mineral species of 7d and 28d are similar, and the peaks of each characteristic are different. From 7d to 28d, the peak values of hydration products increased and that of incomplete hydration minerals decreased. The peak values of the same minerals at the same age were lower than those of SSP, and there was a mineral characteristic peak of hydration product $Ca(OH)_2$. The characteristic peaks of gypsum minerals may be the hydration products or the residues that are not involved in the reaction of the activator. After 28 hydration of activated SSP slurry, the characteristic peak values of periclase mineral that causes the poor stability of SSP was smaller than that of 7d and 28d activated SSP. The results showed that the activator can accelerate the hydration of SSP and effectively digested the components with poor stability.

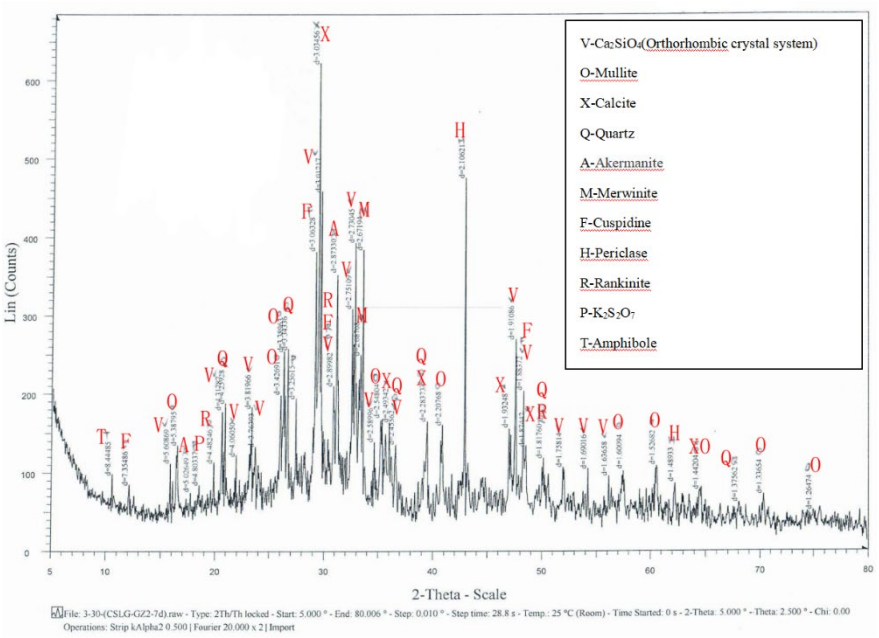

(a) 7d

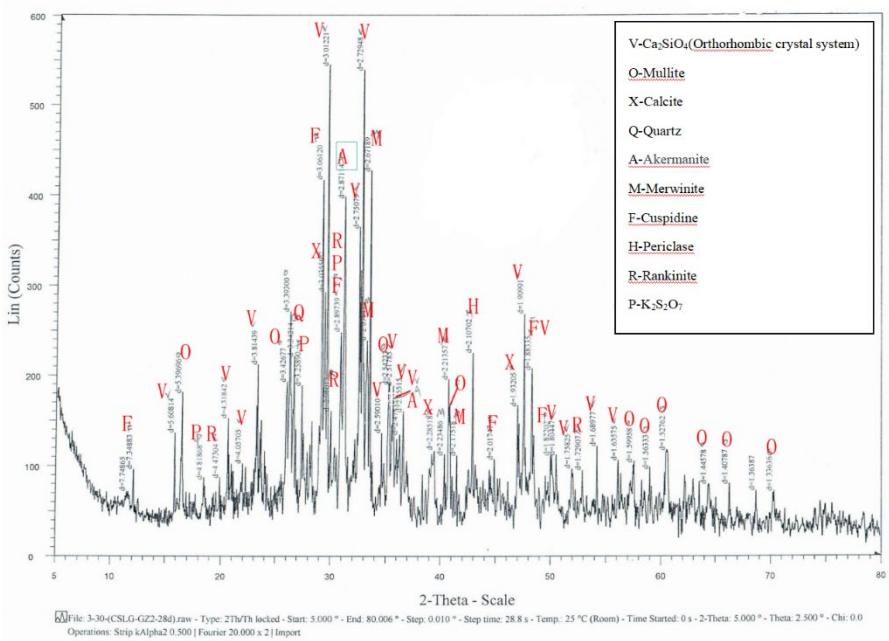

(b) 28d

Fig. 6 XRD diagram of activated SSP slurry

3.3 SEM analysis of SSP cement composite cementitious material

Fig. 7 and Fig. 8 are the SEM images of 7d hydration products of activated SSP cement composite powder and activated SSP slurry. (a) and (b) are the SEM images with different magnifications. It can be seen that the micro morphology of 7d hydration products of activated SSP cement composite powder slurry was not different from that of cement slurry at the same age. However, there are many unhydrated particles on its surface. Compared with the micro-morphology of activated SSP hydration products at the same age, the composite powder contains a large amount of fully developed C-S-H gel and AFT, and a small amount of sheet-shaped $Ca(OH)_2$. AFT grew in a C-S-H gel surface with a white floc, and a sheet-shaped $Ca(OH)_2$ was inlaid in each hydration product for bracket supporting.

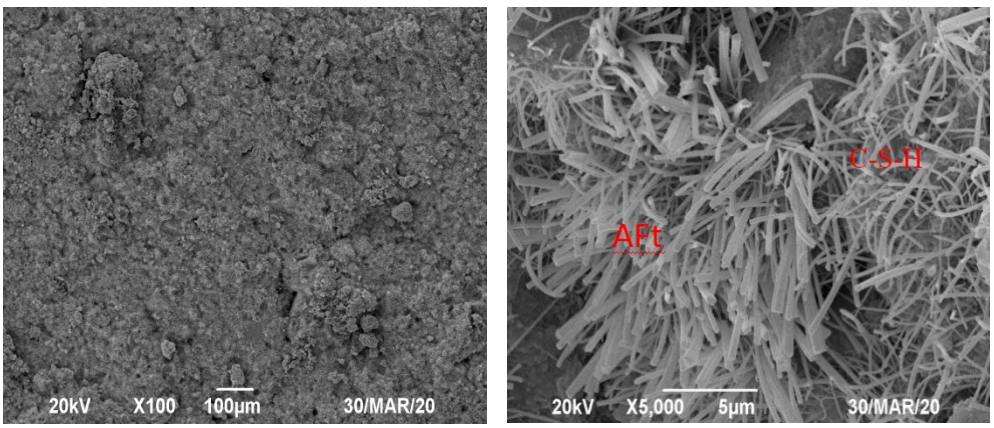

(a) Magnify 100 times (b) Magnify 5000times

Fig. 7 SEM images of hydration products of7d activated SSP cement composite powder slurry

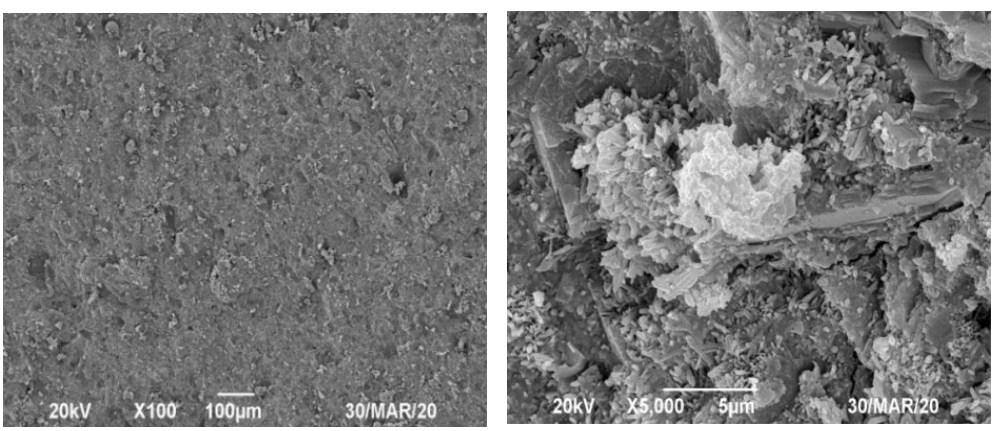

(a) Magnify 100 times (b) Magnify 5000times

Fig.8 SEM images of hydration products of 7d activated SSP slurry

Fig. 9 and Fig. 10 are the SEM images of hydration products of 28d activated SSP cement composite powder and cement slurry, respectively, in which (a)-(d) are the SEM images with different magnifications. It can be seen from Fig. 9(a) and Fig. 10(a) that the micro morphology and compactness of hydration products of 28d activated SSP cement composite powder slurry are not different from that of cement. There are basically no incompletely hydrated particles on the surface. It can be seen from Fig. 9(b), Fig. 9 (c) and Fig. 10(b) that there are a large number of laminated $Ca(OH)_2$ hydration products. The needle-shaped AFt is tightly embedded between $Ca(OH)_2$ and C-S-H flocculant gel and interspersed in AFt with large particle cluster C-A-H. Rosette AFM also interspersed between AFt and covered on $Ca(OH)_2$. Fig. 9 (d) shows that the hydration products are closely connected, interspersed with each other, and fully developed to form a whole. Therefore, the voids between hydration products and the interface between different hydration products will be finally filled with the increase of age. This is beneficial to the formation of strength of SSP cement composite powder.

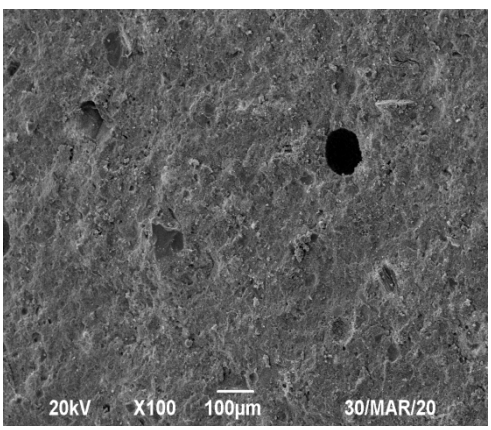

(a) Magnify 100times

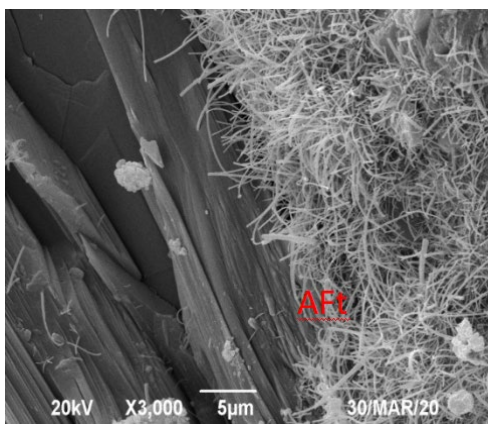

(b) Magnify 3000 times

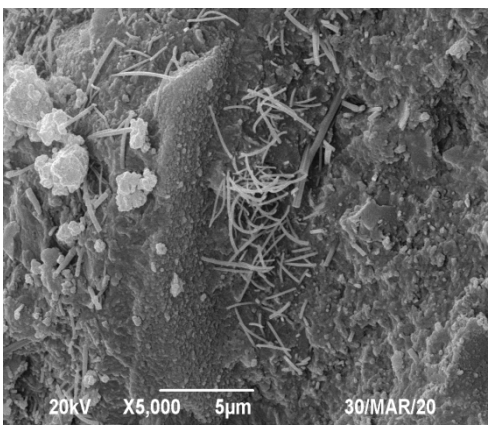

(c) Magnify 5000times

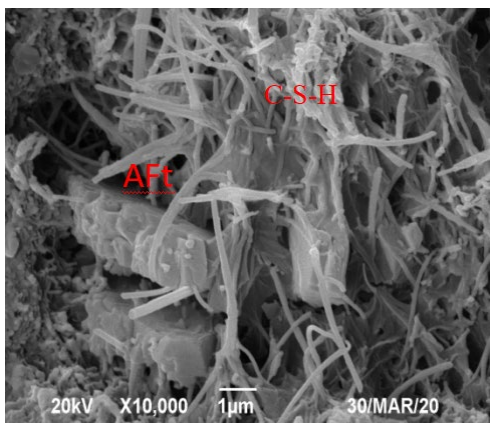

(d) Magnify 10000times

Fig. 9 SEM images of hydration products of 28d activated SSP cement composite powder slurry

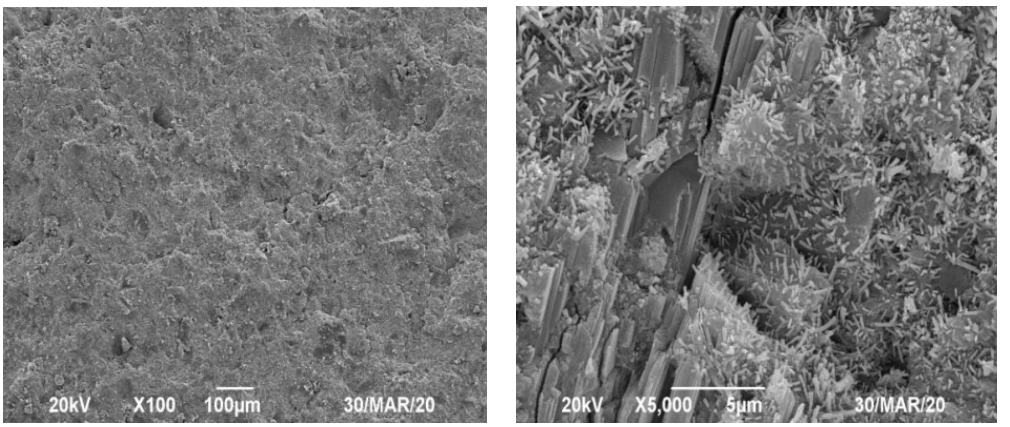

(a) Magnify 5000times (b) Magnify 10000times

Fig. 10 SEM images of 28d hydration products of cement slurry

3.4 Thermogravimetric differential thermal analysis

Fig. 11 and Fig. 12 are the TG-DTG curves of 7d activated SSP cement composite powder and cement slurry. It can be seen that there are two main endothermic peaks for 7d hydration of composite powder slurry and three endothermic peaks for cement slurry. The temperature range of two endothermic peaks of composite powder slurry is consistent with that of cement. That is, 100-200 ℃ corresponds to the early endothermic peak of C-S-H and Aft; 650-750 ℃ corresponds to the late decarburization reaction of C-S-H and AFt with calcium carbonate, while the endothermic peak of about 450 ℃ in cement slurry is the dehydration endothermic peak of $Ca(OH)_2$. This indicates that there is no $Ca(OH)_2$ hydration product when the composite powder is hydrated for 7d, which is consistent with the results of SEM images.

According to the TG diagram, the mass loss of composite powder is 6.02% between 22.6-238.7 ℃. In 33.5-239.4 ℃, the mass loss of cement is 5.50%, indicating that the amount of C-S-H and AFt in the early 7d hydration of composite powder is greater than that of cement. Although the composite powder did not produce $Ca(OH)_2$ for 7d hydration, it was found that the mass loss between ℃ was still 4.31%. Combined with the XRD results, it may be that the mineral mass in the composite powder was lost more than that in the cement. The final mass residues of the composite powder and cement were 84.44% and 80.12%, respectively. This indicates that the mass loss of cement is greater than that of composite powder, and the amount of cement hydration products is more than that of composite powder.

Fig. 13 and Fig. 14 are the TG-DTG curves of 28d activated SSP cement composite powder and cement slurry, respectively. As shown in the figures, for 28d composite powder slurry, there are two endothermic peaks at 370.1 ℃ and 564.4 ℃, respectively, and two mass changes of 241.7-477.4 ℃ and 477.4-621.7 ℃, respectively. This indicates that a small amount of $Ca(OH)_2$ is generated in the 28d hydration of composite powder slurry. Compared with the TG-DTG diagram of cement slurry at the same age, the peak value of cement is sharp and the peaks are small. The mass loss is still large. It shows that the types of hydration products of composite powder are more than that of cement, but the products are less than that of cement.

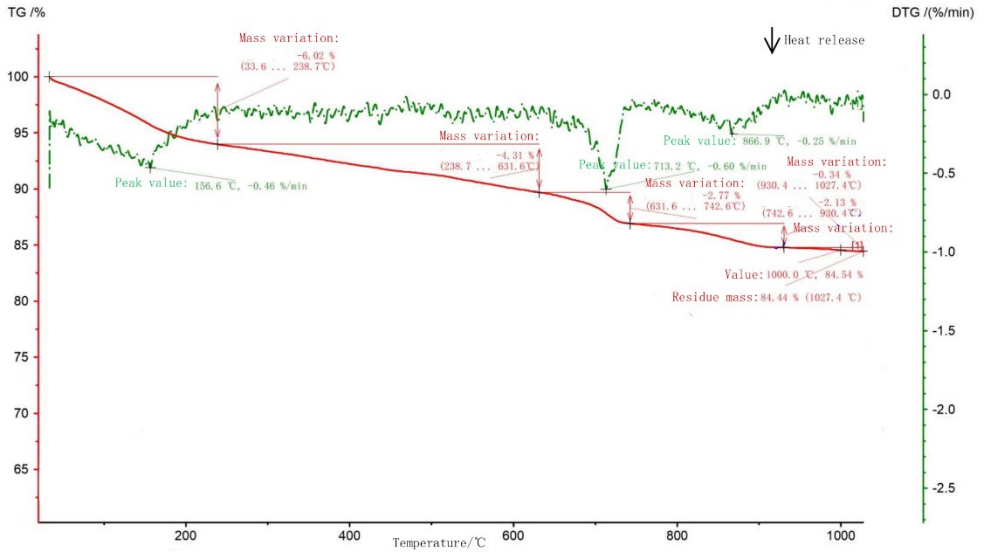

Fig. 11 TG-DTG diagram of 7d hydration of activated SSP cement composite powder slurry

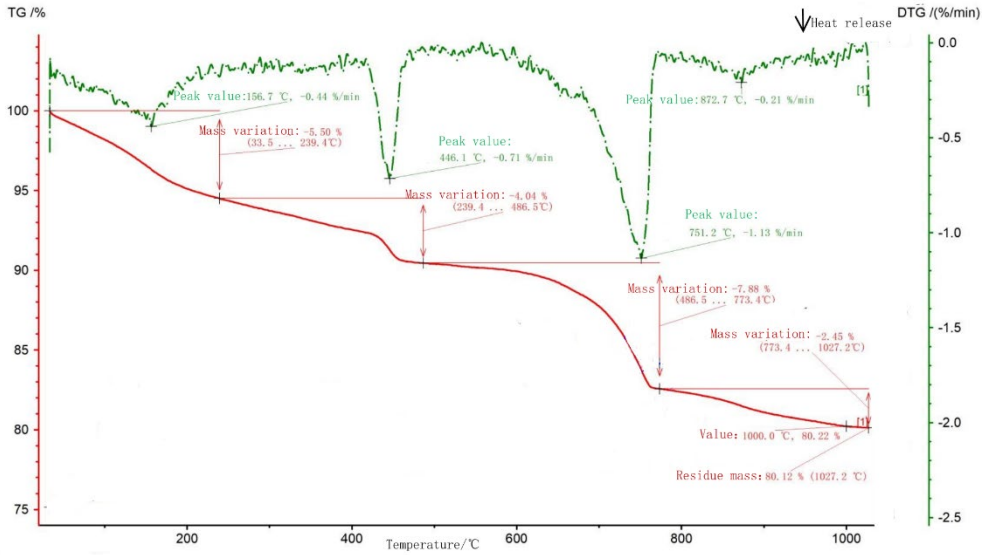

Fig. 12 TG-DTG diagram of 7d hydration of cement slurry

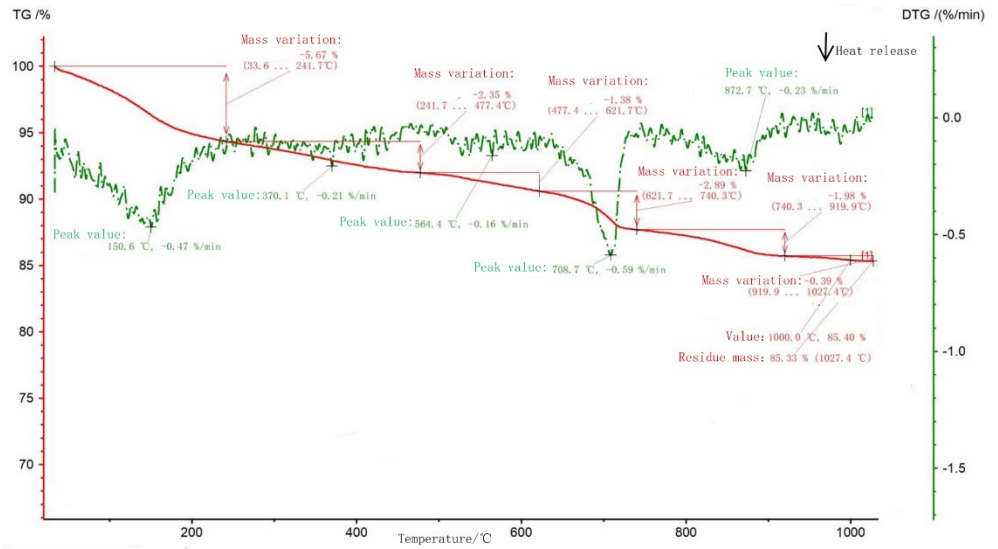

Fig.13 TG-DTG diagram of 28d hydration of activated SSP cement composite powder slurry

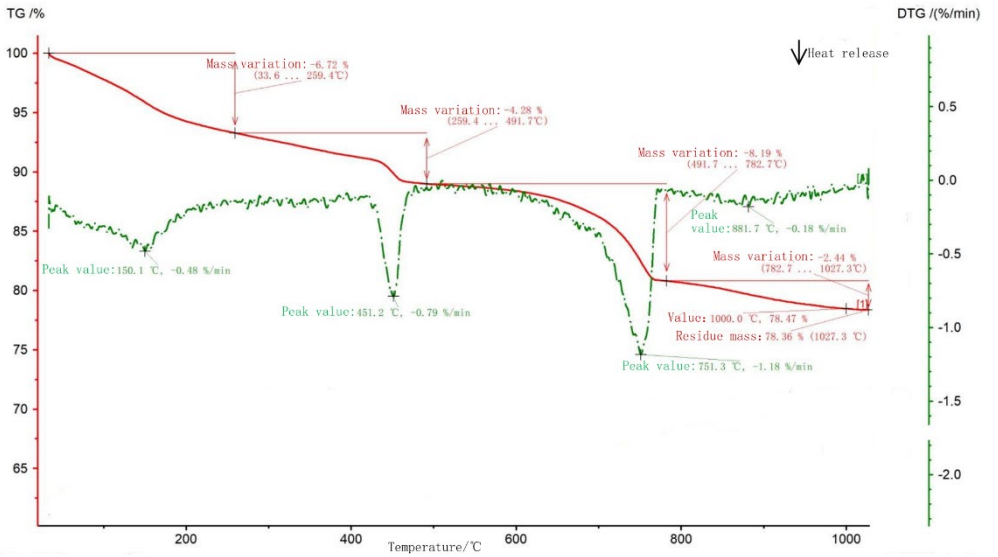

Fig. 14 TG-DTG diagram of 28d hydration of cement slurry

4. CONCLUSION

(1) The composition and ratio of composite activator were optimized through experiments. The optimal ratio of gypsum: silica fume: sodium sulfate: sodium aluminate: self-made activator was 2.5:2.5:1:0.5:0.5.

(2) The micro morphology of 7d hydration products of 30% cement activated steel slag composite powder slurry was not different from the density of cement slurry. However, the unhydrated particles on the surface of composite powder were more than that of cement. At 28d, there were basically no unhydrated particles. The hydration products were closely connected and interspersed with each other, with complete morphological development to form a whole. Under the premise of not losing the later strength, the self-made neutral activator enables the activated steel slag powder to partially replace the cement.

(3) According to the TG-DTG diagram, there were two endothermic peaks for 7d activated SSP cement composite powder slurry, and three endothermic peaks for cement. The composite powder had no endothermic peak corresponding to the temperature of $Ca(OH)_2$. At the age of 7d and 28d, the mass loss of cement was large, and the types of hydration products of composite powder were more than those of cement, but the overall quantity was less. When the activated steel slag powder was hydrated for 28d days, the main mineral phases of the hydration products were dicalcium silicate and tobermorite, and the minerals with the highest characteristic peaks were similar to the cement slurry. The height of the characteristic peak of periclase mineral decreased greatly, the activator promoted the hydration of steel slag powder and digested the free oxides that lead to poor stability.

(4) In the future work, the influence of composite activator on the later durability of cement activated SSP composite powder will be discussed. The later hydration and strength formation mechanism will be studied more deeply and carefully, so as to provide support for the application of composite powder in pavement base.

REFERENCES

[1] Fisher L. V., Barron A. R., The recycling and reuse of steelmaking slags-A review. Resources, conservation and recycling, 2019, 146: p. 244-255.

[2] Dominguez A. G., Valerio Cuadros M. I., Borja Castro L. E., Valencia Bedregal R. A., Santibañez J. F., Suarez S. M., Cabrera Tinoco H., Moreno N.O., Barnes C. H. W., Valladares L., & De Los Santos, Characterization and Mössbauer spectroscopy of steel slag generated in the ladle furnance in SIDERPERU steel plant. Hyperfine Interactions, 2022, 243(1): p. 1-11.

[3] Jiang, Y., & Ling, T. C., Production of artificial aggregates from steel-making slag: Influences of accelerated carbonation during granulation and/or post-curing. Journal of CO2 Utilization, 2020, 36: p. 135-144.

[4] Das, P., Upadhyay, S., Dubey, S., & Singh, K. K., Waste to wealth: Recovery of value-added products from steel slag. Journal of Environmental Chemical Engineering, 2021. 9(4): p. 105640.
[5] Martins, A. C. P., de Carvalho, J. M. F., Costa, L. C. B., Andrade, H. D., de Melo, T. V., Ribeiro, J. C. L., Pedroti, L.G., Peixoto, R. A. F., Steel slags in cement-based composites: An ultimate review on characterization, applications and performance. Construction and Building Materials, 2021, 291: p. 123265.
[6] Lai, M. H., Zou, J., Yao, B., Ho, J. C. M., Zhuang, X., & Wang, Q., Improving mechanical behavior and microstructure of concrete by using BOF steel slag aggregate. Construction and Building Materials, 2021, 277: p. 122269.
[7] Zou, M., Shen, Y., Liu, J. H., Review on application of steel slag powder in cement-based materials. Bulletin of the Chinese ceramic society, 2021, 40(09): p. 2964-2977.
[8] Nunes, V. A., & Borges, P. H., Recent advances in the reuse of steel slags and future perspectives as binder and aggregate for alkali-activated materials. Construction and Building Materials, 2021, 281: p. 122605.
[9] Li, X. F., Doh, S. I., Feng, W. Y., Albtoosh, J. F. A. A., & Chong, B. W., The Mechanical Properties of Concrete Incorporating Steel Slag as Supplementary Cementitious Material. Key Engineering Materials, 2021, 879: p. 81-90.
[10] Li, M. S., Jiang, J.P., Liu, H., Duan, P., Jing, W., Ge, W., & Wang, Z.S., Effects of Lithium Slag and Steel Slag on Mechanical Properties and Microstructure of Cement Paste. Bulletin of the Chinese ceramic society, 2022, 41(06): p. 2098-2107.
[11] Parron-Rubio, M.E., Perez-García, F., Gonzalez-Herrera, A., & Rubio-Cintas, M.D., Concrete properties comparison when substituting a 25% cement with slag from different provenances. Materials (Basel), 2018, 11: p. 1-13.
[12] Raheem, A. A., Olowu, O. A., Hungbo, A. A., & Ibiwoye, E. O., Effects of Water Cement Ratio on Strengths Characteristics of Concrete Produced with Recycled Iron and Steel Slag (RISS) Aggregate. Advances in Science and Technology, 2021, 107: p. 97-112.
[13] Huang, H. R., Liao, Y. S., Qunaynah, S. A., Jiang, G. X., Guo, D. W., & Yuan, W. J., Effect of Steel Slag on Shrinkage Characteristics of Calcium Sulfoaluminate Cement. Materials Science Forum, 2021, 1036: p. 263-276.
[14] Miah, M. J., Ali, M. K., Monte, F. L., Paul, S. C., Babafemi, A. J., & Šavija, B., The effect of furnace steel slag powder on the performance of cementitious mortar at ambient temperature and after exposure to elevated temperatures. Structures, 2021, 33: p. 2811-2823.
[15] Zhou, Y. L., Zheng, Y. C., Li, X. R., Wang, H., Li, R., Influence of pre-treatment process on the grinding efficiency and performance of steel slag. Concrete, 2022, 2: p. 111-115.
[16] Morone, M., Costa, G., Georgakopoulos, E., Manovic, V., Stendardo, S., & Baciocchi, R., Granulation-Carbonation Treatment of Alkali Activated Steel Slag for Secondary Aggregates Production. Waste and Biomass Valorization, 2017. 8: p. 1381-1391.
[17] Fang, Y., Su, W., Zhang, Y., Zhang, M., Ding, X., & Wang, Q., Effect of accelerated precarbonation on hydration activity and volume stability of steel slag as a supplementary cementitious material. Journal of Thermal Analysis and Calorimetry, 2021. 6: p. 1-11.
[18] Shen, W., Liu, Y., Wu, M., Ecological carbonated steel slag pervious concrete prepared as a key material of sponge city. Journal of cleaner production, 2020, 256: p. 120244.

[19] Díaz-Piloneta, M., Terrados-Cristos, M., Álvarez-Cabal, J. V., & Vergara-González, E., Comprehensive Analysis of Steel Slag as Aggregate for Road Construction: Experimental Testing and Environmental Impact Assessment. Materials, 2021. 14(13): p. 3587.

[20] Sun, J., Zhang, Z., Zhuang, S., & He, W., Hydration properties and microstructure characteristics of alkali-activated steel slag. Construction and Building Materials, 2020. 241: p. 118141.

[21] Guan, J., Zhang, Y., Yao, X., Li, L., Zhang, L., & Yi, J., Experimental Study on the Effect of Compound Activator on the Mechanical Properties of Steel Slag Cement Mortar. Crystals, 2021. 11(6): p. 658.